# The Effect of the Interface Structure of Different Surface-Modified Nano-$SiO_2$ on the Mechanical Properties of Nylon 66 Composites

**Xiangmin Xu,[1] Binjie Li,[1] Huimin Lu,[1] Zhijun Zhang,[1] Honggang Wang[2]**

[1]*Key Laboratory for Special Functional Materials, Henan University, Kaifeng, Henan 475000, China*
[2]*State Key Laboratory of Solid Lubrication, Lanzhou Institute of Chemical Physics, Chinese Academy of Sciences, Lanzhou, Gansu 730000, China*

Received 1 March 2007; accepted 10 August 2007
DOI 10.1002/app.27325
Published online 30 October 2007 in Wiley InterScience (www.interscience.wiley.com).

**ABSTRACT:** The nylon 66-based nanocomposites containing two different surface-modified and unmodified $SiO_2$ nanoparticles were prepared by melt compounding. The interface structure formed in different composite system and their influences on material mechanical properties were investigated. The results indicated that the interfacial interactions differed between composite systems. The strong interfacial adhesion helped to increase tensile strength and elastic modulus of composites; whereas, the presence of modification layer in silica surface could enhance the toughness of composites, but the improvement of final material toughness was also correlated with the density of the adhered nylon 66 chains around silica nanoparticles. In addition, the results also indicated that the addition of surface-modified silica nanoparticles has a distinct influence on the nonisothermal crystallization behavior of the nylon 66 matrix when compared with the unmodified silica nanoparticle. © 2007 Wiley Periodicals, Inc. J Appl Polym Sci 107: 2007–2014, 2008

**Key words:** interfaces; mechanical properties; nylon; composite

## INTRODUCTION

In the recent years, the study of polymer-based nanocomposites has attracted much interest in the field of material science. When compared with their neat counterparts, the nanocomposites exhibit superior properties such as enhanced mechanical and thermal properties, improved barrier performance, and flame retardancy.[1–7] However, the application of polymer-based nanocomposites is also confined due to the challenges in fully and uniformly dispersing the nanofillers within the polymer matrix. To obtain better dispersion in polymer matrix, nanofillers are usually pretreated by different surface-modified technology. The use of modified nanoparticles as fillers, which can provide a larger interfacial adhesion region and different surface functional groups, might result in considerably strong interaction with the matrix and improvement of the final material properties. Therefore, the influence of interface structure on the material properties has been paid more attention in the last few years.[8,9]

Nylon 66 is a kind of important engineering plastic; nano-$SiO_2$ is one of the most applied nanofillers in thermoplastic polymer composites. However, for nylon 66/nano-$SiO_2$ composite, there are few reports involving this field, and some reports are mainly focused on nylon 6/nano-$SiO_2$ composite.[10–12] Presently, nylon 6/nano-$SiO_2$ composites have usually been prepared by *in situ* polymerization, in which silica nanoparticles are dispersed in ε-caproamide and aminocapric acid, followed by heat treatment of the reaction mixture to induce polymerization. Using *in situ* polymerization method, Yang et al.[11] found that silica nanoparticles modified with aminobutiric acid were dispersed more homogeneously in the polymeric matrix compared to the fillers, which were not surface modified, and the addition of silica nanoparticles led to an increase in the glass transition temperature and crystallization rate of matrix nylon 6. Moreover, Li et al.[12] achieved the enhancement of the strength and toughness of composites simultaneously, in which silica nanoparticles were pretreated with different coupling agents for the improvement of the matrix-filler interface. Meanwhile, the conception of flexible interfacial layer was proposed, which was considered as the main reason for the improvement of the material mechanical properties.

In this study, to examine the influence of different interface structure on the mechanical properties of composites, three different kinds of surface-modified nano-$SiO_2$ are used and blend with nylon 66 via melt compounding. The possible reactions between silica surface functional groups and nylon 66 are

*Correspondence to:* Z. Zhang (xxm326@gmail.com).

studied by the aid of Fourier transform infrared spectroscopy (FTIR), thermogravimetric analysis (TGA), and transmission electron microscopy (TEM). The influence of different interface structure on the mechanical properties of the composite materials and nonisothermal crystallization behavior is also discussed.

## EXPERIMENTAL

### Materials and sample preparation

Neat nylon 66 (PA66) pellets (EPR27, with relative viscosity of 2.67), were provided by China Shenma Engineering Plastics Co. (PingDingShan, China). Two different surface-modified and unmodified nano-$SiO_2$ used in this study were supplied by Henan Nanomaterial Research Center of Engineering and Technology (JiYuan, China). Modified silicas were prepared by surface-modification *in situ* in aqueous solution. Surface modification of nano-$SiO_2$ *in situ* was a condensationlike polymerization in which the hydrolysis product of sodium metasilicate was used as monomer and 3-aminopropyltriethoxysilane (APS) and hexamethyldisilazane (HMDS) as chain terminator, respectively. First, sodium metasilicate was hydrolyzed to form the silicic acid under the existence of hydrochloric acid. Condensation polymerization happened by anhydration among the hydroxyls of silicic acids at three dimensions, and the Si and O were bonded to each other to form the defective three-dimensional structures by tetrahedron. Large numbers of hydroxyls were left on the surface of silica nanoparticles. In the mean time, APS (or HMDS) was introduced and silanol groups of APS (or trimethylsilyl of HMDS) generated by hydrolysis could react rapidly with hydroxyl groups of $SiO_2$ to form the modification layer on silica surface, as shown in Figure 1. As the organic chains substituted portion of active groups of silica surface and resulted in a steric hindrance, which prevented $SiO_2$ from continuously growing up or agglomerating. By controlling the reaction conditions, we could obtain nano-$SiO_2$ particles ''capped'' with different organic compound.[13,14]

Before melt processing, silica and nylon 66 were dried for 12 h under vacuum at 80 and 100°C, respectively. Nylon 66 nanocomposites with different silica content (up to 5 wt %) were prepared by melt compounding using Brabender twin-screw extruder at 270–280°C with a screw speed of 100 rpm. The pelletized materials were dried and molded in an Engel ES200/45 machine into dumbbell-shaped tensile bars (150 mm × 10 mm × 4 mm) and rectangular bars (50 mm × 6 mm × 4 mm). Impact test were performed on the rectangular bars, and a 45° V-shaped notch (depth = 0.8 mm) was milled in the bars.

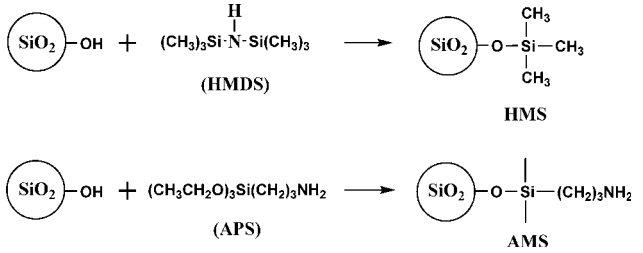


**Figure 1** The schematic illustration of formation mechanism of modified nano-$SiO_2$.

### Isolation of silica from nylon 66/nano-$SiO_2$ composites

To analyze the characterization of interfacial layer, it was necessary to isolate silica from the composites systems. The matrix nylon 66 was removed from the nylon 66/nano-$SiO_2$ composites using formic acid. Formic acid was selected because it could dissolve the matrix nylon 66 well without corroding the interfacial layer on the silica surface. The composites with APS-modified silica nanoparticles and unmodified silica nanoparticles were directly extracted using formic acid, whereas the composites with HMDS-modified silica nanoparticles were difficult to be extracted by formic acid due to superior hydrophobic and oleophilic properties of HMDS-modified silica nanoparticles. So, the mixed solution of formic acid and toluene (mixed proportion 2 : 1) was adopted to extract silica from nanocomposite. After the polymer-based nanocomposites were fully dissolved, the suspension obtained was centrifuged, and the deposition was collected. The procedure was repeated until no more polymers could be detected by FTIR in the residual solution. Finally, the deposition was washed with methanol and dried under vacuum at 100°C.

For the sake of convenience, APS-modified silica nanoparticles, HMDS-modified silica nanoparticles, and unmodified silica nanoparticles were designated hereafter as AMS, HMS, and UMS, respectively, and silica isolated from nylon 66/AMS, nylon 66/HMS, and nylon 66/UMS nanocomposites were labeled as CAMS, CHMS, and CUMS, respectively.

### Interfacial layer characterization

The amount of nylon 66 adhered on silica surface after a removal of matrix nylon 66 from the nanocomposites was measured by TGA using TA 2050 instrument with a heating rate of 10°C/min under nitrogen atmosphere. The FTIR spectra of the isolated silicas from nanocomposites were recorded in KBr pellets on a Nicolet 170 FTIR spectrometer. The morphology of isolated silicas from nanocomposites had been observed by TEM using a JOEL JEM-2010 at an accelerating voltage of 200 kV.

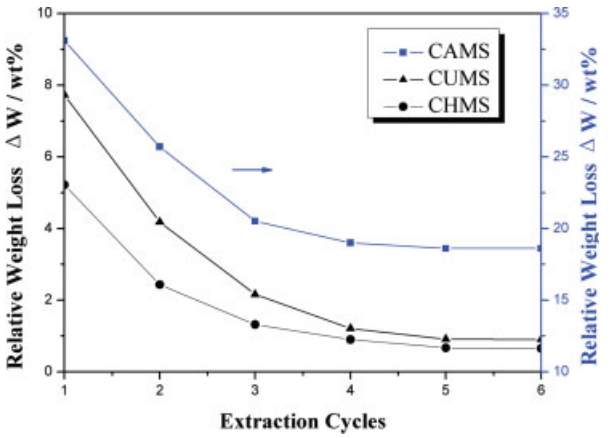


**Figure 2** Extraction cycle dependence of relative weight loss for various nylon 66/nano-$SiO_2$ composites. [Color figure can be viewed in the online issue, which is available at www.interscience.wiley.com.]

### Mechanical characterization

The tensile testing of the composites was conducted on a DY35 universal testing machine (Adamel Lhomargy, France) at room temperature. The tensile tests were performed at a crosshead speed of 20 mm/min. The notched Charpy impact strength was measured with ZBC1400-2 (SANS, China) at a rate of 2.9 m/s. All these tests were conducted at ambient temperature (20–25°C), and an average value of least five repeated tests was taken for each nanocomposites.

### Differential scanning calorimetry

The crystallization behaviors of both neat nylon 66 and nanocomposites were analyzed using differential scanning calorimetry (DSC) (Seiko Instruments, Exstar 6000). The samples of ~5 mg were heated from room temperature (20°C) to 280°C at a rate of 20°C/min, held at 280°C for 5 min to eliminate the heat history, and then quenched in liquid nitrogen. Afterward, the samples were heated to 280°C at 10°C/min under nitrogen atmosphere, held at that temperature for 2 min, and then cooled back to room temperature. Here, by using the heat of fusion for 100% crystalline nylon 66 as 206 J/g, the percentage crystallinity of neat nylon 66 and nanocomposites could be estimated.

## RESULTS AND DISCUSSION

### TGA analysis of silica isolated from nylon 66/ nano-$SiO_2$ composites and original silicas

When nano-$SiO_2$ (modified or unmodified) blended with nylon 66 in twin-screw extruder, surface groups of silica nanoparticles possibly reacted with the matrix nylon 66 and formed adhered nylon 66 layer on $SiO_2$ surface. For investigating the amount of nylon 66 adhered on silica surface, the weight loss of original silica and silica isolated from nanocomposites was measured by TGA. Figure 2 shows the extraction cycle dependence on the relative weight loss $\Delta W$ for various nanocomposites, $\Delta W$ for difference value of weight loss between silica isolated from composite and original silica. The relative weight loss of three different kinds of composites becomes constant after four extraction cycles. The result of six extraction treatment indicates that the amount of adhered nylon 66 is the highest for nylon 66/AMS nanocomposites. The relative weight loss of nylon 66/HMS and nylon 66/UMS nanocomposites is very low (<1), due to weight loss of HMS and UMS approximately equal to that of their extraction products CHMS and CUMS. This clearly indicates that nylon 66 weakly attached to HMS and UMS surface have almost completely removed by the extraction treatment. For nylon 66/AMS nanocomposites, it seems reasonable to consider that a strongly or chemically interfacial adhesion have been formed between AMS nanoparticles and nylon 66 matrix.

### Characteristics of silica isolated from nylon 66/nano-$SiO_2$ composites

To characterize the chemical composition of interfacial layer, silica isolated from the composites were analyzed by FTIR. Figure 3 shows the FTIR spectra of matrix nylon 66, CAMS, CUMS, and CHMS. When compared with neat nylon 66, the spectra of

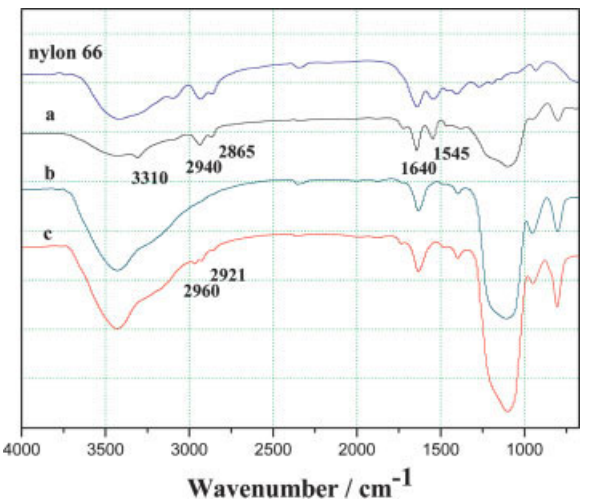


**Figure 3** FTIR spectra of nylon 66 and silicas: (a) CAMS, (b) CUMS, and (c) CHMS. [Color figure can be viewed in the online issue, which is available at www.interscience.wiley.com.]

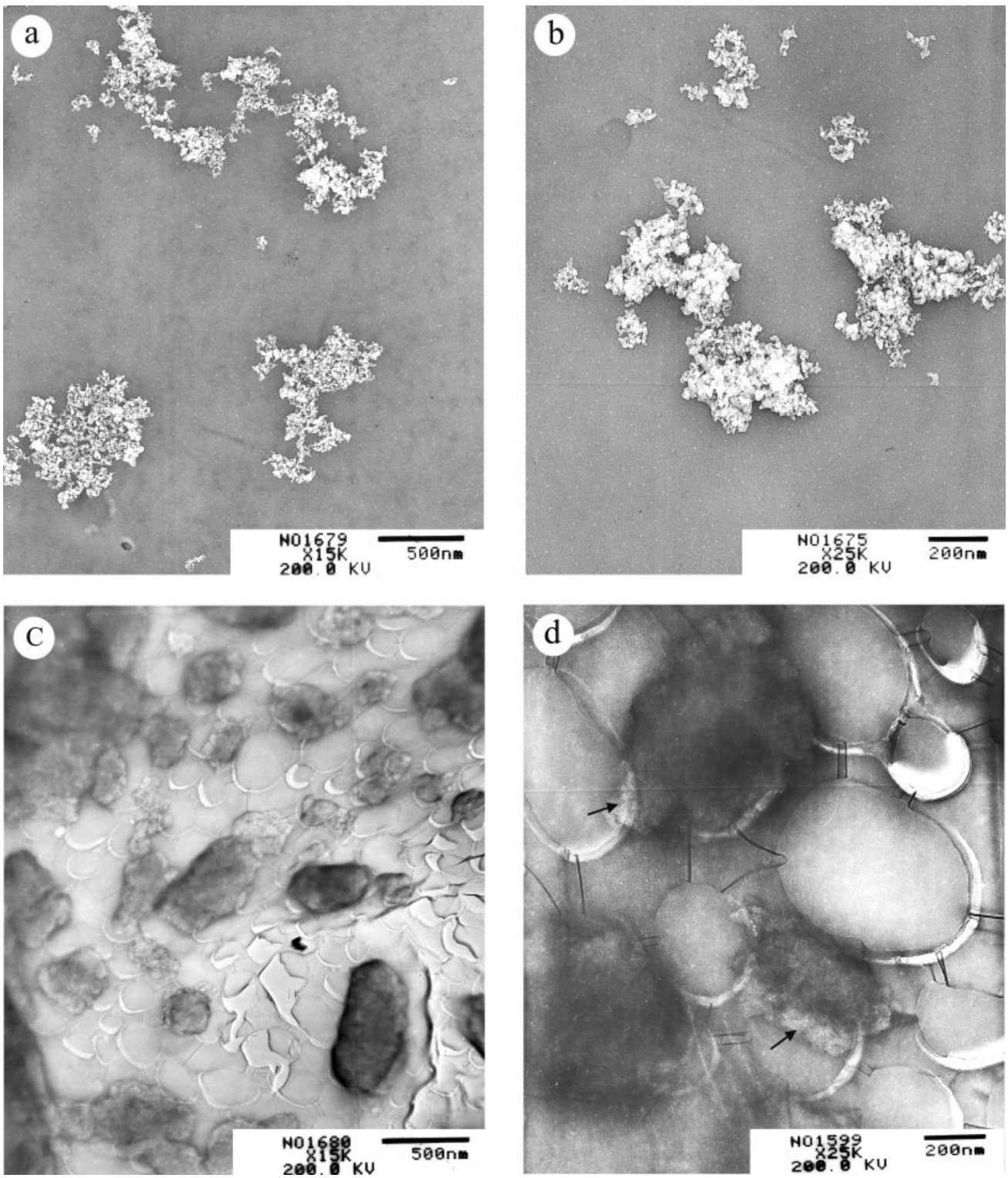


**Figure 4** TEM photographs of silica nanoparticles isolated from various nanocomposites: (a) CUMS, (b) CHMS, (c) and (d) CAMS.

CAMS show the characteristic bands of nylon 66 at 1640 $cm^{-1}$ and 1545 $cm^{-1}$ (amide bands) and 2940 $cm^{-1}$ and 2865 $cm^{-1}$ (C—H bands). Especially, the appearance of N—H characteristic band at 3310 $cm^{-1}$ (hydrogen bonds) further indicates that there is a considerable amount of nylon 66 chains adhered on AMS surface. In contrast, the spectra of CUMS and CHMS do not exhibit characteristic absorption peaks of nylon 66, suggesting that no grafting polymers on silica surface are formed. The FTIR results

are in agreement with that of TGA. The weak peaks at 2800–3000 $cm^{-1}$ (2960 $cm^{-1}$, 2921 $cm^{-1}$) on curve c are attributed to methyl groups of HMS surface. In the preparation of HMS, the trimethylsilys of HMDS generated by hydrolysis reacted with the surface hydroxyl groups of silica and formed the modification layer on the silica surface with short carbon chains. But it is worth noting that a lack of reactive groups in the modification layer results in no chemical bonding formed between HMS nanoparticles and nylon 66 chains, but interacted via hydrogen bonds. The case of UMS is similar to that of HMS, wherein hydrogen bonds are present between silica nanoparticles and matrix nylon 66, and no polymer is chemically grafted to nano-$SiO_2$ surface. So, it is easy to understand why no characteristic absorption peaks of nylon 66 appear on curves b and c.

The TGA and FTIR results were also confirmed by the TEM images of extraction products as illustrated in Figure 4. It can be seen from Figure 4(a,b) that the TEM image of CUMS is analogous with that of CHMS. Isolated silica particles appear in the form of loose agglomerates with the size of about 200 nm or larger, and no nylon 66 is attached to these agglomerates surface, indicating the weak bonding between UMS, HMS, and matrix nylon 66. When compared with CHMS, the agglomeration trend of CUMS is more obvious, which should be correlated with the surface modification of silica. However, the TEM image of CAMS [Fig. 4(c,d)] is apparently different from that of CUMS and CHMS. It clearly displays in Figure 4(c) that nylon 66 is not completely removed by extraction treatment, and some primary particles of AMS are dispersed into the thin layer of nylon 66. In Figure 4(d), the more details of interface between AMS and nylon 66 can be observed. Nylon 66 is intimately adhered to AMS surface, and some fuzzy regions are present in the interface between AMS and nylon 66, as indicated by arrows, revealing that there is a strong interaction at the interface of these two phases.

From the earlier discussion, it can be found that the addition of different surface-modified nanoparticles can bring on dissimilar interfacial layer structure. Figure 5 shows the schematic representation of the interfacial layer for the nylon 66/HMS, nylon 66/UMS, and nylon 66/AMS nanocomposites. In Figure 5(a,b), hydrogen bonding is the only adhesion mode between nanofillers and the matrix, but both have obvious differences. For nylon 66/HMS composite, when the trimethylsilyls were introduced into the silica surface, the activity of surface hydroxyl groups of HMS was hindered due to the effect of interspace obstruction. With the content of surface hydroxyl groups reducing, the amount of hydrogen bonds formed in nylon 66/HMS interface also decreases compared to nylon 66/UMS interface. Furthermore, the existence of the nonpolar modification layer does not also increase the compatibility of matrix and fillers. All these factors result in a decrease in interfacial adhesion strength of nylon 66/HMS, even lower than nylon 66/UMS, which is possible to produce the influence on the mechanical properties of final composites. On the other hand, for nylon 66/AMS composite, the hydrogen bonds and the covalent bonds were formed in nylon 66/AMS interface by the original hydroxyl groups and amino groups on AMS surface reacted with functional groups of nylon 66 during melt process, as shown in Figure 5(c). The appearance of hydrogen bonds and the covalent bonds promoted the formation of strongly adhered interface structure and effectively restricted the motion of nylon 66 molecular at nylon 66/AMS interface. It is evident that this interface structure will help to enhance the interfacial adhesion strength and to improve stress transfer between nanofillers and matrix in composite system.

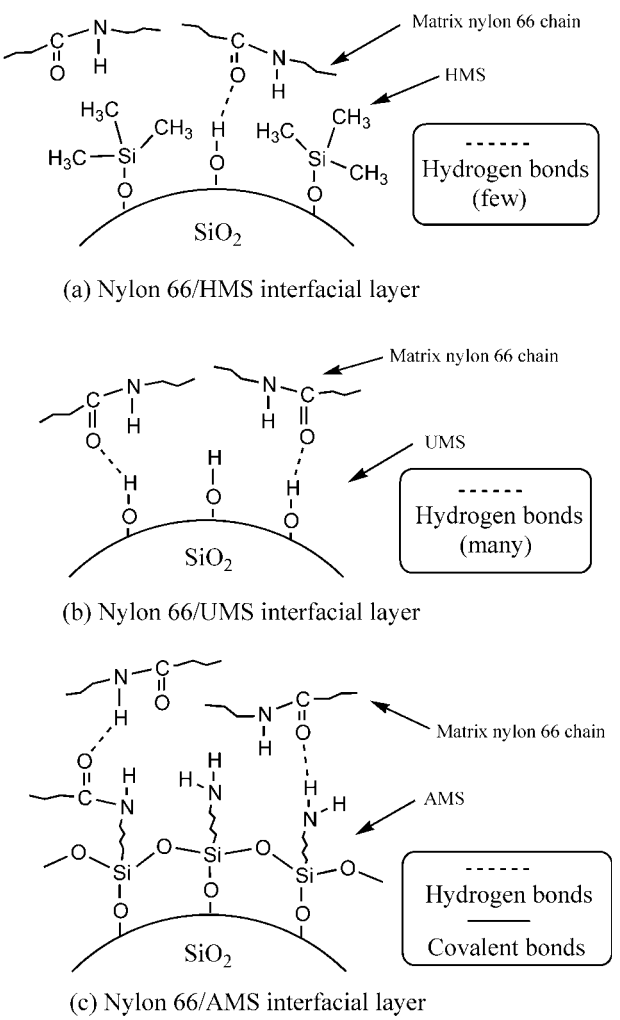


**Figure 5** Schematic representation of the interfacial layer models for the nylon 66/HMS, nylon 66/UMS, and nylon 66/AMS composites.

### The mechanical properties of nylon 66/nano-$SiO_2$ composites

Figure 6 shows the effect of silica content on the mechanical properties of nylon 66/nano-$SiO_2$ composites. It is interesting to note that there is obvious difference in the mechanical properties of the three nanocomposites. When AMS is added into the matrix, tensile strength and Young's modulus of nanocomposite are enhanced. Tensile strength achieves the maximum at the silica content of 3 wt %, and Young's modulus is continuously increased with the increase in silica content. However, to impact strength of nanocomposite, it is different from the tensile performance and shows a slight decrease in trend. When HMS is used, the case is opposite to that of AMS. The tensile strength of composite has an evident decrease, and impact strength is increased significantly compared with neat nylon 66, but Young's modulus of composite rarely changes. With regard to UMS, similarly to the ordinarily used rigid particle, the tensile strength and Young's modulus of composite are enhanced modestly, whereas impact toughness decreased dramatically.

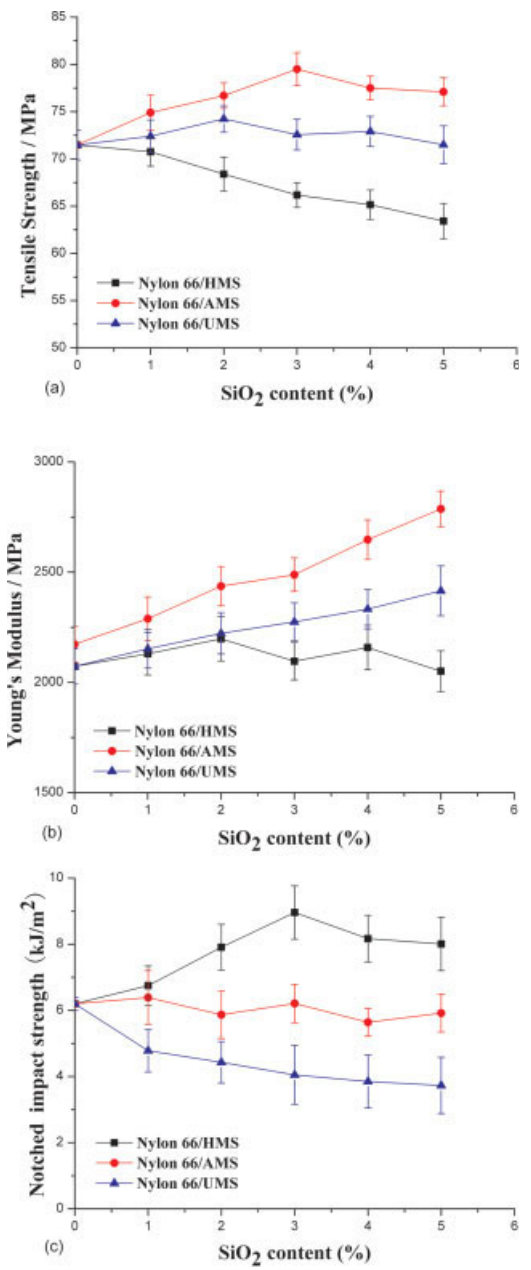


**Figure 6** Mechanical properties of nylon 66/nano-$SiO_2$ composites versus silica content: (a) tensile strength, (b) Young's modulus, and (c) notched impact strength. [Color figure can be viewed in the online issue, which is available at www.interscience.wiley.com.]

It is well known that the mechanical properties of composites are highly related to the filler-matrix interfacial interaction and the size of nanoparticles.[15] As silica particles are easy to aggregate in the process of melt blending and form the agglomeration of random size, the effect of nanoparticle size on material properties has been weakened. Therefore, we consider that interface structure plays an important role in the mechanical properties of composites.

Figure 7 shows the distinct differences in microstructures of silica nanoparticles and matrix interacted in all three nanocomposites. For the nylon 66/AMS nanocomposite, nylon 66 chains are connected to AMS surface by hydrogen bonding and covalent bonding. This interface structure not only can limit the movement of nylon 66 chains and form the high density region of grafting nylon 66 chains around the nanoparticles, but also can effectively transfer load from the matrix to the nanoparticles. Therefore, after AMS nanoparticles are added into the matrix, tensile strength and Young's modulus of composite are enhanced markedly. However, impact strength of composite is not improved simultaneously as expected and exhibits a slight decrease in trend. The change is different from the other reports,[12] which is perhaps the result that the effect of the flexible interfacial layer on silica surface formed by the silane-coupling agent is in competition with the effect of the density of nylon 66 chains around the nanoparticles, as shown in Figure 7(a). The increase of grafting polymer density stiffens the matrix, whereas flexible interfacial layer is beneficial to the improvement of material toughness.[15] It can be seen from the impact test result of nylon 66/AMS nanocomposite, in this study, that the effect of the high density region of nylon 66 around nanoparticles is possibly greater than the effect of flexible interfacial layer on the material toughness, consequently leading to a slight decrease of impact strength. But it is noted that impact strength of nylon 66/AMS nanocomposite is still higher than that of nylon 66/UMS nanocomposite, due to the existence of flexible interfacial layer. For the nylon 66/HMS nanocomposite, few hydrogen bonding in interfacial layer and low nylon 66 chains density around the nanoparticles result into a

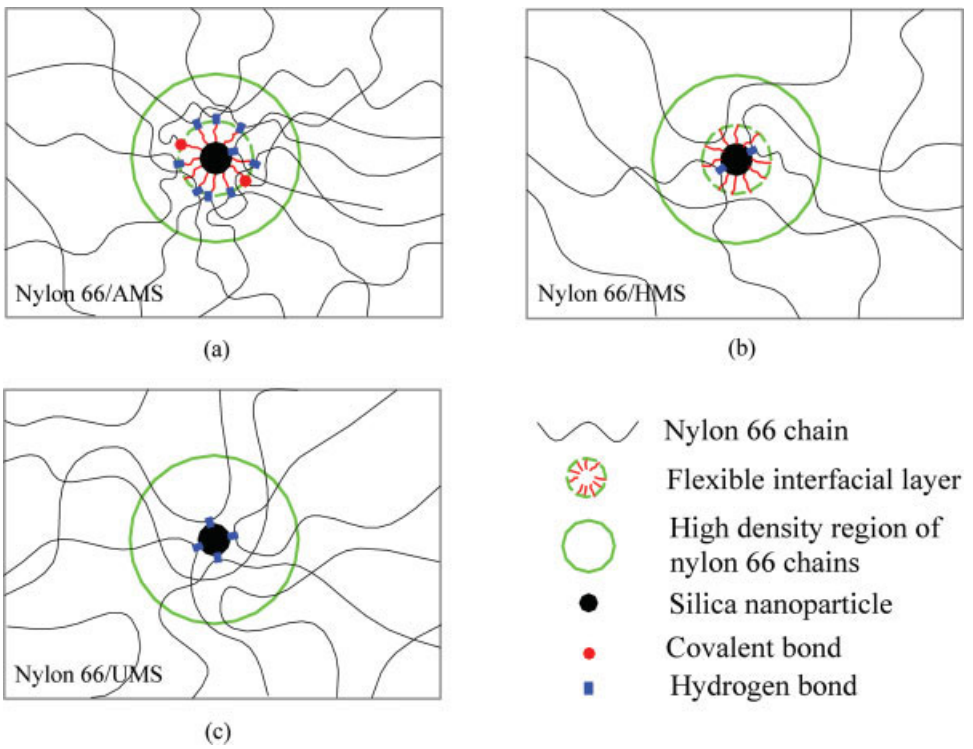


**Figure 7** Schematic illustrations of microstructures of silica nanoparticles and matrix nylon 66 interacted in all three nanocomposites. [Color figure can be viewed in the online issue, which is available at www.interscience.wiley.com.]

lower interfacial adhesion strength, though nanoparticle-matrix interface adhesion can be increased by the entanglement between short carbon chains on HMS surface and matrix nylon 66 chains [Fig. 7(b)]. In comparison with the nylon 66/AMS nanocomposite, the structure differences of interfacial layer are primary reason that tensile strength of nylon 66/HMS composite decreases, as well as the change of elastic modulus is not obvious. However, flexible interfacial layer and lower density of nylon 66 chains around the nanoparticles make for the improvement of material impact toughness. The mechanism can be ascribed to the energy absorption and hindering effect on crack propagation by the nylon 66/HMS interphase. As to the nylon 66/UMS nanocomposite, a certain amount of polymer attached to the silica surface via hydrogen bonds promotes the enhancement of the tensile strength and elastic modulus, whereas more severe aggregation phenomenon of UMS particles during melting blend and absence of flexible interfacial layer result in an obvious decrease of impact strength of nanocomposite.

### Differential scanning calorimetry analyzing

Table I gives some DSC characteristic parameters of nylon 66 and nylon 66/nano-$SiO_2$ composites, wherein the content of silica is 3 wt %. It can be seen that nylon 66 has a melting temperature $T_m$ at 258.7°C, whereas $T_m$ of all three nanocomposites occurs at slightly lower temperatures than that of nylon 66. This phenomenon may be related with the reduction in crystallite size in the presence of nanofillers.[16,17] The same case also appears in the DSC cooling process of nylon 66 and nanocomposites, in which the crystallization temperature $T_c$ of nanocomposites is lower than that of nylon 66. The decease in $T_c$ of nanocomposites may be attributed to the lowering in the nylon 66 molecule mobility when silica nanoparticles are introduced.[18] For UMS, the effect of its addition on the motion of polymer chain segments is limited due to surface unmodification of silica nanoparticles. So, the $T_c$ of nylon 66/UMS nanocomposite is very close to that of nylon 66. In contrast with UMS, the addition of nano-$SiO_2$ with

**TABLE I**
**DSC Characteristic Parameters and Percentage Crystallinity of Nylon 66 and Nylon 66/Nano-$SiO_2$ Composites**

| Samples | $T_m$ (°C) | $T_c$ (°C) | $T_{1/2}$ (min) | $\Delta H_m$ (J/g) | $\chi_c$ (%) |
|---|---|---|---|---|---|
| Nylon 66 | 258.7 | 230.7 | 0.43 | 57.34 | 27.8 |
| Nylon 66/HMS | 256.5 | 228.3 | 0.40 | 58.41 | 28.4 |
| Nylon 66/UMS | 256.1 | 230.6 | 0.44 | 56.24 | 27.0 |
| Nylon 66/AMS | 256.7 | 228.5 | 0.32 | 59.48 | 28.9 |

$T_m$, melting temperature; $T_c$, crystallization temperature; $t_{1/2}$, the half-time of crystallization; $\Delta H_m$, the heat of fusion; $\chi_c$, crystallinity.

modification layer (AMS and HMS) has a greater influence on crystallization temperature, and a distinct decrease in $T_c$ can be observed, implying major hindrance of modification layer to motion of nylon 66 chain segments. The half-time of crystallization $t_{1/2}$ of nylon 66 and nanocomposites are also given in Table I. At the cooling rate of 10°C/min, nylon 66 and nylon 66/UMS nanocomposite have the highest value of $t_{1/2}$, while nylon 66/AMS nanocomposite has the lowest, and nylon 66/HMS nanocomposite is the intermediate. Generally speaking, the shorter the half-time of crystallization, the faster will be the rate of overall crystallization.[19] It is clear that AMS and HMS significantly increase the crystallization rate and exhibit a strong nucleating ability, whereas the case of UMS is different from that of AMS and HMS, and the lower crystallization rate reveals the weaker nucleating ability of UMS. The result of $t_{1/2}$ indicates from another angle that the surface modification facilitates filler-inducing crystallization of nylon 66. The difference of AMS and HMS in $t_{1/2}$ value also reflects the influence of different surface modification on the crystallization rate and nucleating effect. Despite the addition of surface-modified silica enhances the nucleating ability of the matrix and increases the crystallization rate, it is worthy to note that there is only a subtle difference in the crystallinity of nylon 66/AMS, nylon 66/HMS nanocomposites, and neat PA66. We know that the crystallization process is governed by two processes, diffusion and nucleation. Obviously, the incorporation of surface-modified silica nanoparticles has influence on these two terms. On the one hand, silica nanoparticles with modification layer can effectively limit the movement of nylon 66 chains and hinder the diffusion process of polymer chain segments; on the other hand, it acts as a nucleating agent to increase the crystallization rate of matrix material.[20] The result of two effects acting simultaneously is, in this study, that the crystallinity of nylon 66/AMS and nylon 66/HMS nanocomposites does not show a distinct change compared with that of neat PA66. As for UMS, it can be seen from above analyses that its addition has a negative effect on the diffusion process and nucleation process of nylon 66, and so the crystallinity of nylon 66/UMS nanocomposite shows a decreasing trend. However, on the whole, the changes in the crystallinity of nanocomposites are not very evident with the addition of different type of silica nanoparticles. The variety of crystallinity, conversely, indicates that the improvement of mechanical properties of nanocomposites is mainly due to the effect of nanofillers.

## CONCLUSION

Nylon 66/nano-$SiO_2$ composites are prepared by melt blending, in which silica nanoparticles have different surface characteristics. The microstructures on the silica surface after a removal of nylon 66 from nanocomposites are studied by TGA, FTIR, and TEM. The results show that nylon 66 chains are chemically grafted onto the AMS surface, whereas UMS and HMS connect with nylon 66 matrix by hydrogen bonds. Three different interfacial structures formed between nanofillers and matrix result in different mechanical properties of nanocomposites. Owing to the presence of flexible interfacial layer, the addition of HMS and AMS, to some extent, can improve the material toughness, but the enhancement of final material toughness is also related to the density of nylon 66 chains grafted to nanoparticles surface. In fact, whether the matrix toughened depends on the competition between the effect of flexible interfacial layer and the effect of the density of nylon 66 chains around silica nanoparticles. The tensile performance of nanocomposites is in close relationship with the nature of the adhered polymer on the nanoparticles surface. High-interfacial adhesion strength is beneficial to the enhancement of the strength and modulus of composites due to well stress transfer between nanofillers and matrix. In addition, DSC analysis indicates that the incorporation of various surface-modified nano-$SiO_2$ has obvious influence on the nonisothermal crystallization behavior of nylon 66.

## References


1. Han, B.; Ji, G. D.; Wu, S. S.; Shen, J. Eur Polym J 2003, 39, 1641.
2. Alexandre, M.; Dubois, P. Mater Sci Eng R 2000, 28, 1.
3. Yoon, P. J.; Fornes, T. D.; Paul, D. R. Polymer 2002, 43, 6727.
4. Yano, K.; Usuki, A.; Okada, A.; Kurauchi, T.; Kamigaito, O. J Polym Sci Part A: Polym Chem 1993, 31, 2493.
5. Messersmith, P. B.; Giannelis, E. P. J Polym Sci Part A: Polym Chem 1995, 33, 1047.
6. Hu, Y.; Wang, S.; Ling, Z.; Zhuang, Y.; Chen, Z.; Fan, W. Macromol Mater Eng 2003, 288, 272.
7. Schmidt, D.; Shah, D.; Giannelis, E. P. Curr Opin Solid State Mater Sci 2002, 6, 205.
8. Rong, M. Z.; Zhang, M. Q.; Pan, S. L.; Friedrich, K. J Appl Polym Sci 2004, 92, 1771.
9. Buggy, M.; Bradley, G.; Sullivan, A. Compos A 2005, 36, 437.
10. Reynaud, E.; Jouen, T.; Gautheir, C.; Vigier, G. Polymer 2001, 42, 8759.
11. Yang, F.; Ou, Y. C.; Yu, Z. Z. J Appl Polym Sci 1998, 69, 355.
12. Li, Y.; Yu, J.; Guo, Z. X. J Appl Polym Sci 2002, 84, 827.
13. Li, X. H.; Cao, Z.; Liu, F.; Zhang, Z. J.; Dang, H. X. Chem Lett 2006, 35, 1.
14. Li, X. H.; Cao, Z.; Zhang, Z. J.; Dang, H. X. Appl Surf Sci 2006, 22, 7856.
15. Jordan, J.; Jacob, K. I.; Tannenbaum, R.; Sharaf, M. A.; Jasiuk, I. Mater Sci Eng A 2005, 393, 1.
16. Jimenez, G.; Ogata, N.; Kawai, H.; Ogihara, T. J Appl Polym Sci 1997, 64, 2211.
17. Liu, X. H.; Wu, Q. J.; Berglund, L. A. Polymer 2002, 43, 4967.
18. Kuo, M. C.; Huang, J. C.; Chen, M. Mater Chem Phys 2006, 99, 258.
19. Mehta, S.; Deopura, B. L. J Therm Anal Calorim 1993, 40, 597.
20. Dasari, A.; Yu, Z. Z.; Yang, M.; Zhang, Q. M.; Xie, X. L.; Mai, Y. W. Compos Sci Technol 2006, 66, 3097.